

Host *Akkermansia muciniphila* Abundance Correlates With Gulf War Illness Symptom Persistence via NLRP3-Mediated Neuroinflammation and Decreased Brain-Derived Neurotrophic Factor

Neuroscience Insights
Volume 15: 1–15
© The Author(s) 2020
Article reuse guidelines:
sagepub.com/journals-permissions
DOI: 10.1177/2633105520942480



Diana Kimono^{1*}, Dipro Bose^{1*}, Ratanesh K Seth¹, Ayan Mondal¹,
Punnag Saha¹, Patricia Janulewicz², Kimberly Sullivan²,
Stephen Lasley³, Ronnie Horner⁴, Nancy Klimas⁵
and Saurabh Chatterjee¹

¹Environmental Health and Disease Laboratory, NIEHS Center for Oceans and Human Health on Climate Change Interactions, Department of Environmental Health Sciences, University of South Carolina, Columbia, SC, USA. ²Department of Environmental Health, Boston University School of Public Health, Boston, MA, USA. ³Department of Cancer Biology and Pharmacology, University of Illinois College of Medicine, Peoria, IL, USA. ⁴Department of Health Services Policy and Management, University of South Carolina, Columbia, SC, USA. ⁵Department of Clinical Immunology, College of Osteopathic Medicine, Nova Southeastern University, Fort Lauderdale, FL, USA.

ABSTRACT: Neurological disorders are commonly reported among veterans who returned from the Gulf war. Veterans who suffer from Gulf War illness (GWI) complain of continued symptom persistence that includes neurological disorders, muscle weakness, headaches, and memory loss, that developed during or shortly after the war. Our recent research showed that chemical exposure associated microbial dysbiosis accompanied by a leaky gut connected the pathologies in the intestine, liver, and brain. However, the mechanisms that caused the symptoms to persist even 30 years after the war remained elusive to investigators. In this study, we used a rodent model of GWI to investigate the persistence of microbiome alterations, resultant chronic inflammation, and its effect on neurotrophic and synaptic plasticity marker BDNF. The results showed that exposure to GW chemicals (the pesticide permethrin and prophylactic drug pyridostigmine bromide) resulted in persistent pathology characterized by the low relative abundance of the probiotic bacteria *Akkermansia muciniphila* in the gut, which correlated with high circulatory HMGB1 levels, blood-brain barrier dysfunction, neuroinflammation and lowered neurotrophin BDNF levels. Mechanistically, we used mice lacking the NLRP3 gene to investigate this inflammasome's role in observed pathology. These mice had significantly decreased inflammation and a subsequent increase in BDNF in the frontal cortex. This suggests that a persistently low species abundance of *Akkermansia muciniphila* and associated chronic inflammation due to inflammasome activation might be playing a significant role in contributing to chronic neurological problems in GWI. A therapeutic approach with various small molecules that can target both the restoration of a healthy microbiome and decreasing inflammasome activation might have better outcomes in treating GWI symptom persistence.

KEYWORDS: Dysbiosis, *Akkermansia muciniphila*, BDNF, RAGE, 3-nitrotyrosine, peroxyxynitrite, inflammasomes, NLRP3

RECEIVED: May 31, 2020. **ACCEPTED:** June 25, 2020.

TYPE: Gulf War Illness (GWI) and Nervous System Disorders - Original Research

FUNDING: The author(s) disclosed receipt of the following financial support for the research, authorship, and/or publication of this article: Funding for this project was provided by DoD-IIRFA grant: W81XWH1810374 and VA merit award I01 CX001923-01 to Saurabh Chatterjee; W81XWH-16-1-0556 to Dr Stephen Lasley; W81XWH-13-2-0072 to Dr Kim Sullivan. This material is based upon work supported (or supported in part) by the Department of Veterans Affairs, Veterans Health Administration, Office of Research and

Development vide grant no. CX001923-01 to Saurabh Chatterjee. Chatterjee is a 5/8th employee with the US Department of Veterans Affairs.

DECLARATION OF CONFLICTING INTERESTS: The author(s) declared no potential conflicts of interest with respect to the research, authorship, and/or publication of this article.

CORRESPONDING AUTHOR: Saurabh Chatterjee, Environmental Health and Disease Laboratory, NIEHS Center for Oceans and Human Health on Climate Change Interactions, Department of Environmental Health Sciences, University of South Carolina, Columbia, SC 29208, USA. Email: schatt@mailbox.sc.edu

Introduction

Neurological disorders are commonly reported among veterans who returned from the Gulf war (GW) of 1990–1991.^{1–3} Afflicted veterans complain of problems including neuralgias, migraine headaches, muscle weakness and coordination, and memory problems.^{2,4,5} These issues occur in combination with other Gulf War illness (GWI) symptoms, and their pathology is not very well understood. Most veterans who suffer from GWI developed their symptoms during or shortly after the war, and these symptoms persist 30 years later. Although the causes of these symptoms are difficult to pinpoint, epidemiological studies have established a compelling link between these symptoms in different GW veteran cohorts and

environmental exposures which occurred during the war, or chemicals that were applied to the warriors before or shortly after the war.^{6–8} Such exposures include dust from desert storms, depleted uranium, combustion byproducts from oil wells, possible chemical weapons, pesticides, vaccines, and prophylactic medicines such as pyridostigmine bromide (PB).^{9–12}

In recent years, research has focused on studying symptoms as well as elucidating mechanisms of these disorders, using GW veteran cohorts as well as animals and in vitro studies. For example, Van Riper et al¹³ reported widespread disruption in white matter microstructure distribution across brain regions involved in the processing and modulating chronic pain. James et al found that there was a significant positive correlation between C-reactive protein (CRP), pain, and neurocognitive mood in GW veterans. Another study by Abou-Donia et al¹⁴ reported

*Diana Kimono and Dipro Bose have equal contribution.



elevated autoantibodies to neurons and other brain cells, eg, tau proteins, glial acidic fibrillary protein (GFAP), and myosin basic protein (MBP) which indicate neuronal injury or gliosis in GW veterans. In other recent animal studies, Zakirova et al¹⁵ found cognitive deficits in mice several weeks after treatment with GW chemicals, and these deficits were associated with increased astrogliosis and a reduction in synaptophysin in mouse hippocampi and cerebral cortex. Furthermore, Madhu et al¹⁶ found that cognitive impairments which persisted 10 months post-exposure to GW chemicals were associated with increased density of activated microglia and astrocytes in rats and inflammation with elevated levels of HMGB1 in the cerebral cortex.

These studies provide evidence that exposure to GW chemicals plays a significant role in the persistence of neurological dysfunction. This may generally be through the disruption of neuronal networks, reactive glia, which fuel inflammation or weak neuronal growth and neuroplasticity. Many neurological disorders such as Parkinson's disease (PD), Alzheimer's disease (AD), bipolar disorders, and neuropathic pain¹⁷⁻²¹ are associated with decreased levels of neurotrophins or impairments in their signaling pathways.^{22,23} These disorders also commonly present with chronic neuroinflammation.²⁴⁻²⁶ Brain-derived neurotrophic factor (BDNF) is the most prevalent neurotrophins in the brain and has been very widely studied in several diseases and brain functions.^{23,27} It is produced by neurons, and it plays crucial functions in neuroplasticity, growth, and survival of neurons.²⁸

To date, our previous research has focused mainly on the possible role of an altered microbiome (bacteriome and virome) in contributing to a persistent inflammatory phenotype, in acute models of GWI.²⁹⁻³² We proposed that exposure to GW chemicals alters the microbiome in rodents, which then drives inflammation through the production of immunostimulatory particles, ie, damage-associated molecular pattern (DAMPs) and pathogen-associated molecular patterns (PAMPs). These DAMPs may then continuously trigger inflammation in different organ systems. Although our results largely supported our hypothesis, we were still limited in knowing whether the observed changes and mechanisms in the microbiome and associated chronic inflammation due to an altered microbiome indeed persisted.

In this present study, we used a persistence rodent model of GWI in which mice were exposed to GW chemicals for 2 weeks (representing the war phase) after which no further GW chemicals were applied for the next 20 weeks (to represent 20 years after the war). We then investigated the persistence of microbiome alterations, chronic inflammation, and its effect on neuronal health (BDNF levels). We further used an NLRP3 KO mouse to study its potential role of this inflammasome as a primary contributor to the observed neuroinflammation.

Materials and Methods

Materials

We purchased PB and permethrin from Sigma-Aldrich (St. Louis, MO). Anti-RAGE, anti-Claudin 5, anti-HMGB1,

anti-IL-1 β , and anti-ASC-2 were purchased from Santacruz Biotechnology (Dallas, TX), Anti-BDNF from cell signaling technology (Danvers, MA), while anti-NLRP3, anti-3-nitrotyrosine, anti-IL-6, anti-IL-18, anti-TMEM 119 primary antibodies were purchased from Abcam (Cambridge, MA). Species specific biotinylated conjugated secondary antibodies and Streptavidin-HRP (Vectastain Elite ABC kit) were purchased from Vector Laboratories (Burlingame, CA). Fluorescence conjugated (Alexa Fluor) secondary antibodies, ProLong Diamond antifade mounting media with DAPI and Pierce LAL chromogenic endotoxin quantitation kit were bought from Thermo Fisher Scientific (Waltham, MA) while enzyme-linked immunosorbent assay (ELISA) kits were purchased from ProteinTech (Rosemond, IL). Unless otherwise specified, all other chemicals used were purchased from Sigma. Paraffin-embedding of tissue and sectioning were done by AML laboratories (Baltimore, MD) and at the Instrument Resources Facility, University of South Carolina School of medicine (Columbia, SC). Microbiome analysis was done by Cosmos ID (Rockville, MD).

Animal experiments

Adult (10 weeks old) wild type male (C57BL/6J mice) and NLRP3 deficient adult (10 weeks) male (B6N.129-Nlrp3tm3Hhf/J) mice were purchased from the Jackson Laboratories (Bar Harbor, ME). Mice experiments were implemented in accordance with National Institutes of Health (NIH) guidelines for humane care and use of laboratory animals and local Institutional Animal Care and Use Committee (IACUC) standards. All procedures were approved by the University of South Carolina at Columbia, SC. Mice were housed individually and fed on a chow diet at 22°C to 24°C with a 12 h light/12 h dark cycle. All mice were sacrificed after animal experiments had been completed. Right after anesthesia, blood from the mice was drawn using cardiac puncture, to preserve serum for further experimentation. Their brains were removed immediately, and the frontal cortex dissected out and was fixed using Bouin's fixative solution. We also collected the fecal pellets and luminal contents for microbiome analysis.

Treatments and rodent model of Gulf War illness

Mice were exposed to GW chemicals (PB and permethrin) based on established rodent models of GWI with some modifications.^{31,33-35} The treated mice group (GWP) and NLRP3KO (GWP-NLRP3KO) mice group were dosed tri-weekly for 2 weeks with PB (2 mg/kg) and permethrin (200 mg/kg) by oral gavage, after which no further treatments with GW chemicals were applied, and mice were fed on a normal chow diet for 20 weeks. The control group (CONT) of mice received vehicle (0.6% dimethyl sulfoxide in phosphate-buffered saline [PBS]) by oral gavage as in other experiments above. Each group had a starting sample size of n=6 until the end of the experiments. All experimental mice had an average starting weight of

26.5 grams and a final weight of 33.5 grams at the end of the study. There was no significant difference of weight difference between controls and Gulf War chemical treated groups over the 20 week period.

Microbiome analysis

Microbiome analysis was done by CosmosID (Rockville, MD, USA) from fecal pellets and luminal contents, which were collected from the animals of each group after sacrifice. DNA isolation, sequencing, and analysis of gut microbiome were performed according to vendor optimized protocol. Briefly, DNA was isolated from fecal samples using the ZymoBIOMICS Miniprep kit, following the manufacturer's instructions. 16S sequencing was carried out on the V3V4 (341 nt–805 nt) region of the 16S ribosomal RNA (rRNA) gene with a 2-step polymerase chain reaction (PCR) strategy. First, PCR was performed using 16S-optimized primer set to amplify the V3–V4 regions of 16S ribosomal DNA (rDNA) within the metagenomic DNA. Then the PCR products from the previous steps were mixed at equal proportions and used as templates in the second step to produce Illumina dual-index libraries for sequencing, with both adapters containing an 8bp index allowing for multiplexing. The dual-indexed library amplification products are purified using Ampure beads (Beckman Coulter). Library quantification was performed using Qubit dsDNA HS assay (Thermo Fisher) and qualified on a 2100 Bioanalyzer instrument (Agilent) to show a distribution with a peak in the expected range. A final qualitative PCR (qPCR) quantification was performed before loading onto a MiSeq (Illumina) sequencer for PE250 (v2 chemistry). The sequences for each sample were then run on the 16S pipeline of the CosmosID GENIUS software, and results were analyzed.

Laboratory Methods

Immunohistochemistry

The fixed brain tissues were embedded in paraffin and sliced into 5 μ M thick sections. These sections were deparaffinized following optimized standard protocols. Epitope retrieval solution and steamer (IHC-Word, Woodstock, MD) were used for epitope retrieval for deparaffinized sections. About 3% H_2O_2 was used for the recommended time to block the endogenous peroxidase. After serum blocking, the primary antibodies were applied at recommended and optimized concentrations. Species-specific biotinylated conjugated secondary antibodies and streptavidin conjugated with HRP were used to implement antigen-specific immunohistochemistry. 3,3'-Diaminobenzidine (DAB) (Sigma Aldrich, St Louis, MD) was used as a chromogenic substrate. Mayer's hematoxylin solution (Sigma Aldrich) was used as a counterstain. Sections were washed between steps using PBS 1 \times . Finally, stained sections were mounted in Simpo-mount (GBI Laboratories, Mukilteo, WA). Tissue sections were observed using Olympus BX63 microscope (Olympus, America). CellSens software from Olympus America (Center Valley, PA) was used for morphometric analysis of images.

Table 1. Primer sequences.

PRIMER	SEQUENCE
mm-Claudin 5	Sense: TTCGCCAACATTGTCGTCC Antisense: TCTTCTTGTCTAGTCGCCG
mm-18S	Sense: TTCGAACGAACGTCTGCCCTATCAA Antisense: ATGGTAGGCACGGCGATA

Immunofluorescence staining

Paraffin-embedded sections were deparaffinized using the standard protocol. Epitope retrieval solution and steamer were used for epitope retrieval of sections. Primary antibodies were used at recommended dilutions. Species-specific secondary antibodies conjugated with Alexa Fluor (633-red and 488-green) were used at advised dilution. In the end, the stained sections were mounted using prolong diamond antifade reagent with DAPI. Sections were observed under Olympus fluorescence microscope BX63 using 20X, 40X, 60X objective lens.

Real-time quantitative PCR

Total RNA was isolated from frontal cortex tissue homogenization in TRIzol reagent (Invitrogen, Carlsbad, CA, USA) according to the manufacturer's instructions and purified with the use of RNeasy mini kit columns (Qiagen, Valencia, CA, USA). Complementary DNA (cDNA) was synthesized from purified RNA (1 μ g) using iScript cDNA synthesis kit (Bio-rad, Hercules, CA, USA) following the manufacturer's standard protocol. Real-time qPCR (qRT-PCR) was performed with the gene-specific primers using Sso Advanced SYBR Green Supermix and CFX96 thermal cycler (Bio-rad, Hercules, CA, USA). Threshold cycle (Ct) values for the selected genes were normalized against respective samples internal control 18S. Each reaction was carried out in triplicates for each gene and for each sample. The relative fold change was calculated by the 2 $^{-\Delta\Delta Ct}$ method. The sequences for the primers used for real-time PCR are provided in Table 1.

Endotoxin level detection by *Litmus Amebocyte* Lysate assay

Serum bacterial endotoxin levels (EU/mL) were detected using the Pierce LAL Chromogenic Endotoxin Quantification Kit (Waltham, MA) according to the manufacturer's instructions. Briefly, serum samples were obtained from mice and diluted 1:80 with endotoxin-free water. The endotoxins were then quantified.

Western blot analysis

About 30 mg of tissue from each brain tissue sample was immediately homogenized in 300 μ L of RIPA buffer with protease and phosphatase inhibitors cocktail (Pierce, Rockford, IL) using slow speed mechanical homogenizer. The homogenate was centrifuged, and the supernatant was collected and saved for

experimental use. About 30 µg of denatured protein from each sample was loaded per well of Novex 4% to 12% bis-tris gradient gel (Life Technologies, Carlsbad, CA) and subjected for standard sodium dodecyl sulfate polyacrylamide gel electrophoresis (SDS-PAGE). Separated protein bands were transferred to nitrocellulose membrane using precut nitrocellulose/filter paper sandwiches (Bio-Rad, Hercules, CA) and Trans-Blot Turbo transfer system (Bio-Rad) using 30-minute transfer protocol. Furthermore, blots were blocked with 3% bovine serum albumin solution prepared in Tris-buffered saline with 0.05% tween-20 (TBS-T). Primary antibodies were used at recommended dilutions in 1.5% blocking buffer and incubated overnight at 4°C. Species-specific anti-IgG secondary antibody conjugated with HRP were used at recommended dilutions in 1% blocking buffer and incubated for 2 h at room temperature. Pierce ECL Western Blotting substrate (Thermo Fisher Scientific Inc, Rockford, IL) was used in dark to develop the blot. Finally, the blot was imaged using G:Box Chemi XX6 (Syngene imaging systems) and subjected to densitometry analysis using Image J software.

ELISA

Serum IL-1β, IL-6, and TNF-α were estimated using ELISA kits from ProteinTech (Rosemont, IL) according to manufacturer protocol.

Statistical analysis

We conducted calculations for each experimental condition prior to initiation of the study. Preliminary data confirmed that the sample size was enough to achieve a minimum statistical power of 0.80 at an alpha of 0.05. One-way analysis of variance (ANOVA) was used with post hoc comparisons among different exposure conditions or treatments (eg, least significant differences [LSD] and Bonferroni correction) to compare means among multiple groups. Student *t* tests was used to compare means between two groups at the termination of treatment. Correlative associations were tested using Pearson's correlation coefficient analysis with Graph pad prism software (GraphPad Software Inc, La Jolla, CA). A *p* value of less than *p*=0.05 was considered statistically significant.

Results

Gulf War chemical exposure results in a decreased relative abundance of Akkermansia muciniphila, which negatively correlates with increased circulatory HMGB1 levels

Our previous studies have strongly suggested that exposure to GW chemicals alters the microbiome and these alterations may contribute to the persistence of GWI symptoms through the release of DAMPs and PAMPs.³⁰⁻³² In this study, we analyzed the microbiome for alterations in specific bacterial species that have a notable role in inflammation persistence in

chronic diseases of the gut, metabolic reprogramming, and neuronal deficiencies. We analyzed 10 distinct bacterial species that had a fold change difference in abundance and has been found to contribute to inflammation and metabolic responses (Figure 1A) We found that mice treated with GW chemicals (GWP) had a significantly lower abundance of *A muciniphila* (significant, Figure 1B, **P*= .008; *n* = 5), *Bacteroides thetaiotomicron*, and *Dorea Sp* (not significant) when compared with mice treated with only vehicle control (Figure 1A). Notably, *A muciniphila* has been associated with several health benefits.³⁶⁻³⁸ Furthermore, we found that mice which were treated with GW chemicals (GWP) had significantly higher HMGB1 levels in their serum compared with mice treated with vehicle control only (CONT) **P*= .034; *n* = 6 (Figure 1C and D). We then carried out statistical analyses to determine whether the increased levels of HMGB1 were related to the observed decreased relative abundance of *A muciniphila*. In Figure 1E, we found that there was a negative correlation between *A muciniphila* abundance and circulatory HMGB1 levels (Pearson's *r* = -0.50; *R*² COD = 0.255).

Exposure to GW chemicals is associated with blood-brain barrier tight junction protein dysregulation, and the changes persist five months after exposure

The study by Abou-Donia et al¹⁴ suggests the presence of a leaky blood-brain barrier (BBB) among veterans who returned from the GW, and this may be a portal for immunostimulatory particles such as DAMPS and PAMPS to continuously fuel neuroinflammation. We studied the messenger RNA (mRNA) and protein expression levels of Claudin 5, the major tight junction protein in the complex that makes up the BBB. We found that GWP mice also exhibited significantly lower Claudin 5 mRNA and protein levels compared with vehicle control treated mice (CONT) *P*= .042 and *P*= .03; *n* = 6 (Figure 2A to C). Furthermore, we studied the levels of Claudin 5 in the BBB by observing colocalizations between Claudin 5 and CD31, a marker for endothelial cells that make up the lining of the blood vessels (Figure 2D and E). We found that there was a significant decrease in the number of colocalizations (yellow spots) constituting Claudin 5 and CD31 in GWP mice compared with controls (CONT) (*P*= .04; *n* = 6). This result points to the fact that at least one major component of BBB integrity is repressed at the protein level, paving the way for possible dysfunctional BBB, and this may lead to the passage of DAMPS such as HMGB1 leaking into the brain and triggering several immune responses.

GW chemical exposure is associated with persistent activation of microglia via the HMGB1-RAGE pathway resulting in increased reactive oxygen species and triggering of the NLRP3 inflammasome

Chronic neurological disorders such as AD and PD are characterized by activation of immune cells such as microglia, the

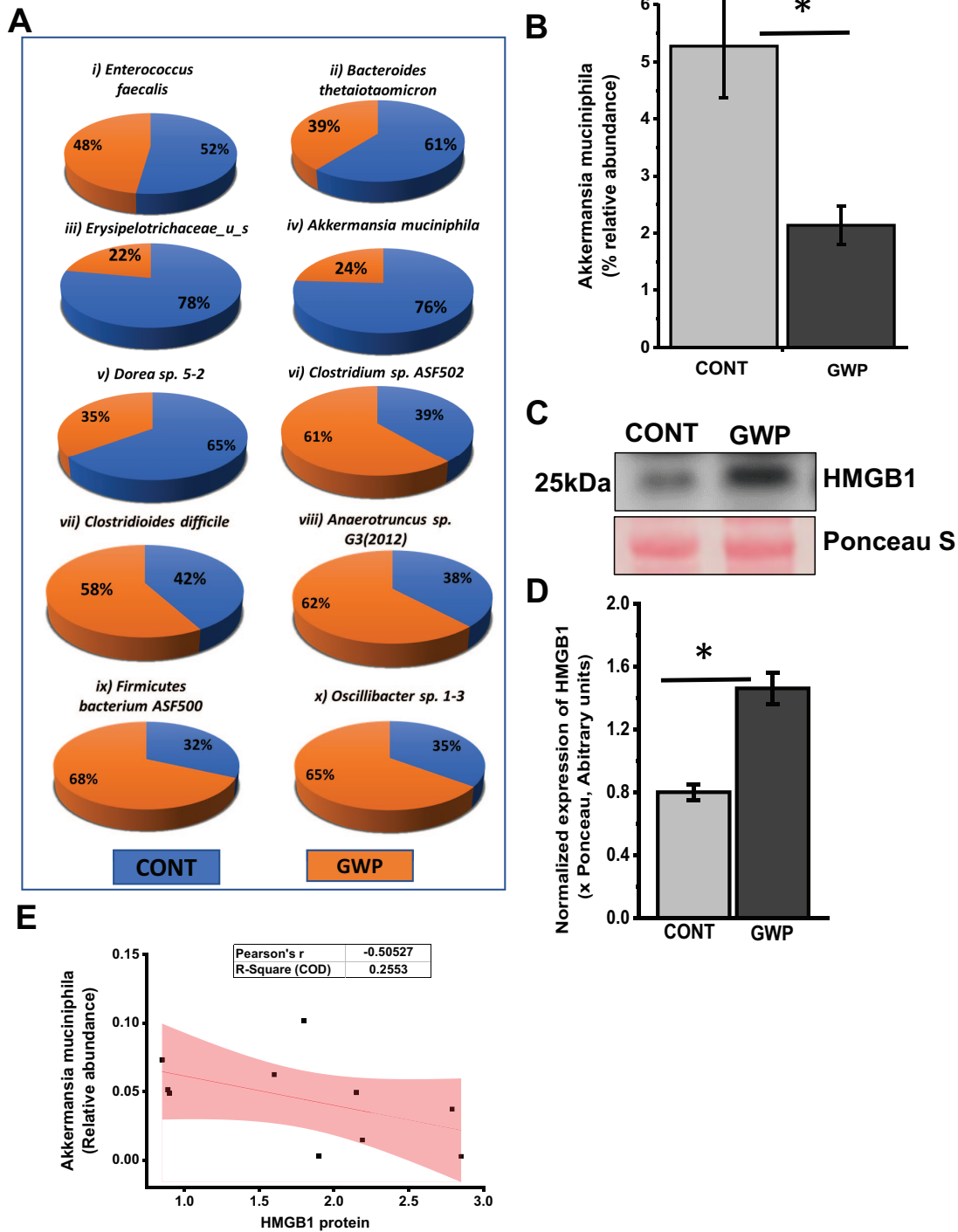


Figure 1. Exposure to GW chemicals results in decreased relative abundance of *Akkermansia muciniphila* and chronic high levels of circulatory HMGB1. (A) Percentage abundance of gut bacteria species. Percentage abundance of 10 most abundant species in the gut bacteriome are represented comparing GW chemical treated groups (GWP) to vehicle control treated group groups (CONT). Data are represented as the mean of 6 mice per group. (B) Percentage relative abundance of *A. muciniphila*. Percentage relative abundance was determined from duplicate fecal samples of 5 mice per group treated with GW chemicals (GWP) compared with mice treated with vehicle control only (CONT). Data are represented as mean \pm SEM ($*P < .05$; $n=5$). (C) Serum HMGB1 levels. Western blot of HMGB1 levels in serum for mice treated with GW chemicals (GWP) compared with mice treated with vehicle control (CONT) only. Data are represented as mean \pm SEM. (D) Densitometry of HMGB1 immunoblots, normalized against Ponceau red ($*P < .05$; $n=6$). (E) Relationship between *A. muciniphila* and circulatory HMGB1 levels. A correlative analysis was carried out to determine how *A. muciniphila* is related to serum HMGB1 levels. We found a negative correlation between *A. muciniphila* and serum HMGB1 levels (Pearson's $r = -0.50$; R^2 COD = 0.255 shaded area represents 95% confidence bands). GW indicates Gulf War; SEM, standard error of the mean; COD, coefficient of dispersion.

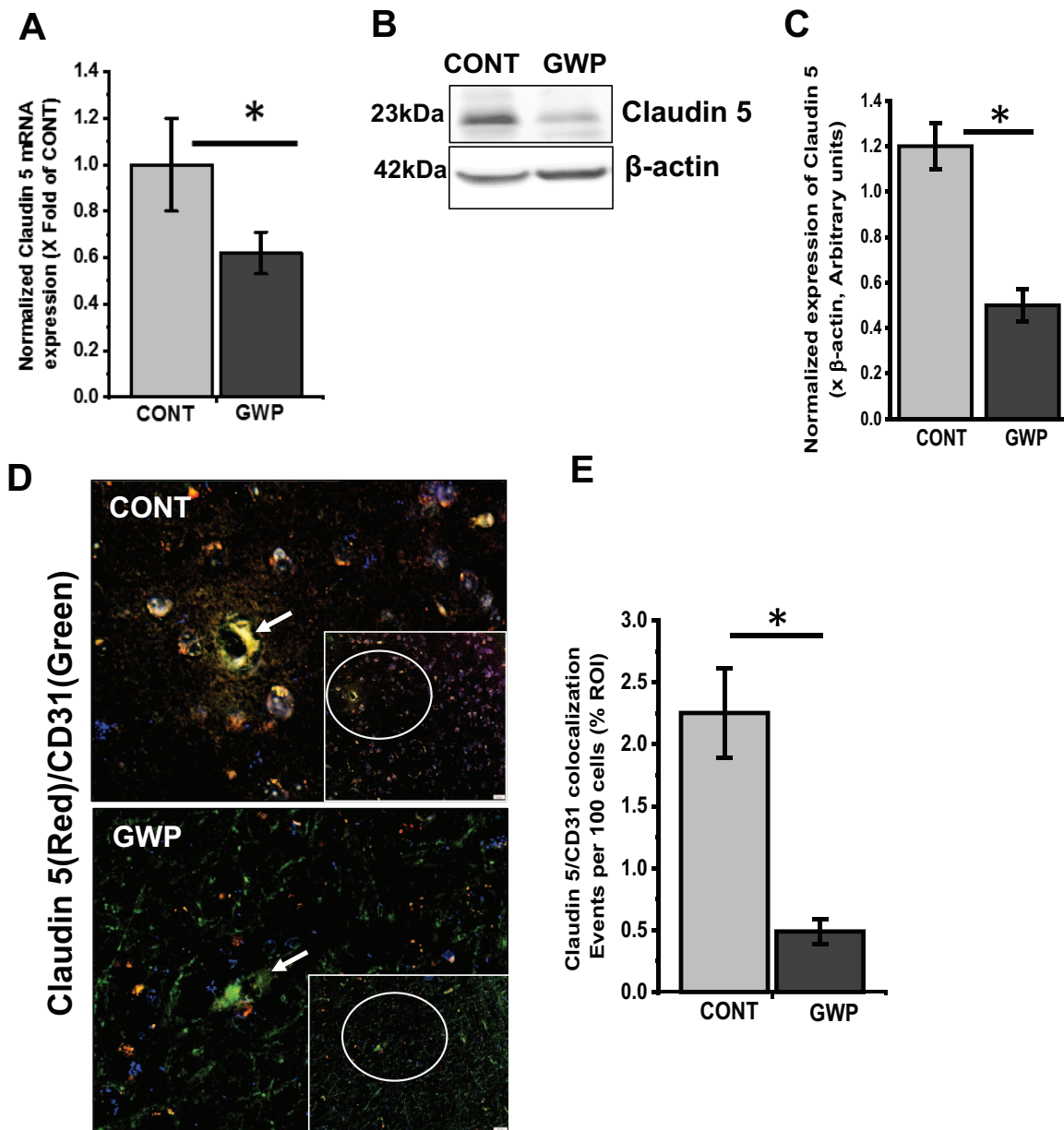


Figure 2. Exposure to GW chemicals is associated with altered Claudin 5 levels in the frontal cortex. (A) Claudin 5 mRNA levels in the frontal cortex: mRNA levels of Claudin 5 as studied by RTqPCR show that mice exposed to GW chemicals (GWP) had significantly decreased Claudin 5 mRNA levels compared with mice treated with vehicle control only (CONT). (B) Claudin 5 protein levels in frontal cortex. Western blot analysis of Claudin 5 protein levels in CONT and GWP treated mice. (C) Morphometry analysis of Claudin 5 immunoblots, normalized against β -actin ($*P < .05$; $n=6$). Data are represented as mean \pm SEM. (D) Representative immunofluorescence micrographs of the blood-brain barrier showing colocalization of tight junction protein Claudin 5 (labeled in red) and endothelial cell marker CD31 (labeled in green) as yellow spots around a BBB (magnification 60 \times and scale bar 10 μ m) and DAPI stained nucleus (labeled in blue). See Supplemental Figure S2 for images of separate channels. Inset (magnification 40 \times and scale bar 20 μ m) shows the whole micrograph field, from which the main image was obtained. (E) Quantitative morphometry analysis of colocalizations for every 100 cells represented as % ROI ($*P < .05$; $n=6$). Data are represented as mean \pm SEM. BBB indicates blood-brain barrier; GW, Gulf War; SEM, standard error of the mean; ROI, region of interest.

resident macrophages of the brain.³⁹ These cells may be activated by the presence of pathogens or DAMPS, such as HMGB1. We studied the protein expression levels of activated microglia marker TMEM119. The results showed that there was a significant increase in activated microglia in the frontal cortex of mice treated with GW chemicals (GWP) compared with controls (CONT) ($*P = .02$; $n=6$) (Figure 3A and B) even after 3 months of exposure. Furthermore, we found

that there was evidence of activated HMGB1-RAGE signaling, as indicated by colocalization events. Figure 3C and D shows a significantly high expression of RAGE protein levels ($*P = .04$; $n=6$) and subsequent increased RAGE-HMGB1 colocalizations ($*P = .001$; $n=6$) in GWP mice compared with controls (Figure 3E and F). RAGE is a receptor, which binds several ligands including HMGB1. Interaction of HMGB1-RAGE can lead to increasing reactive oxygen species (ROS)

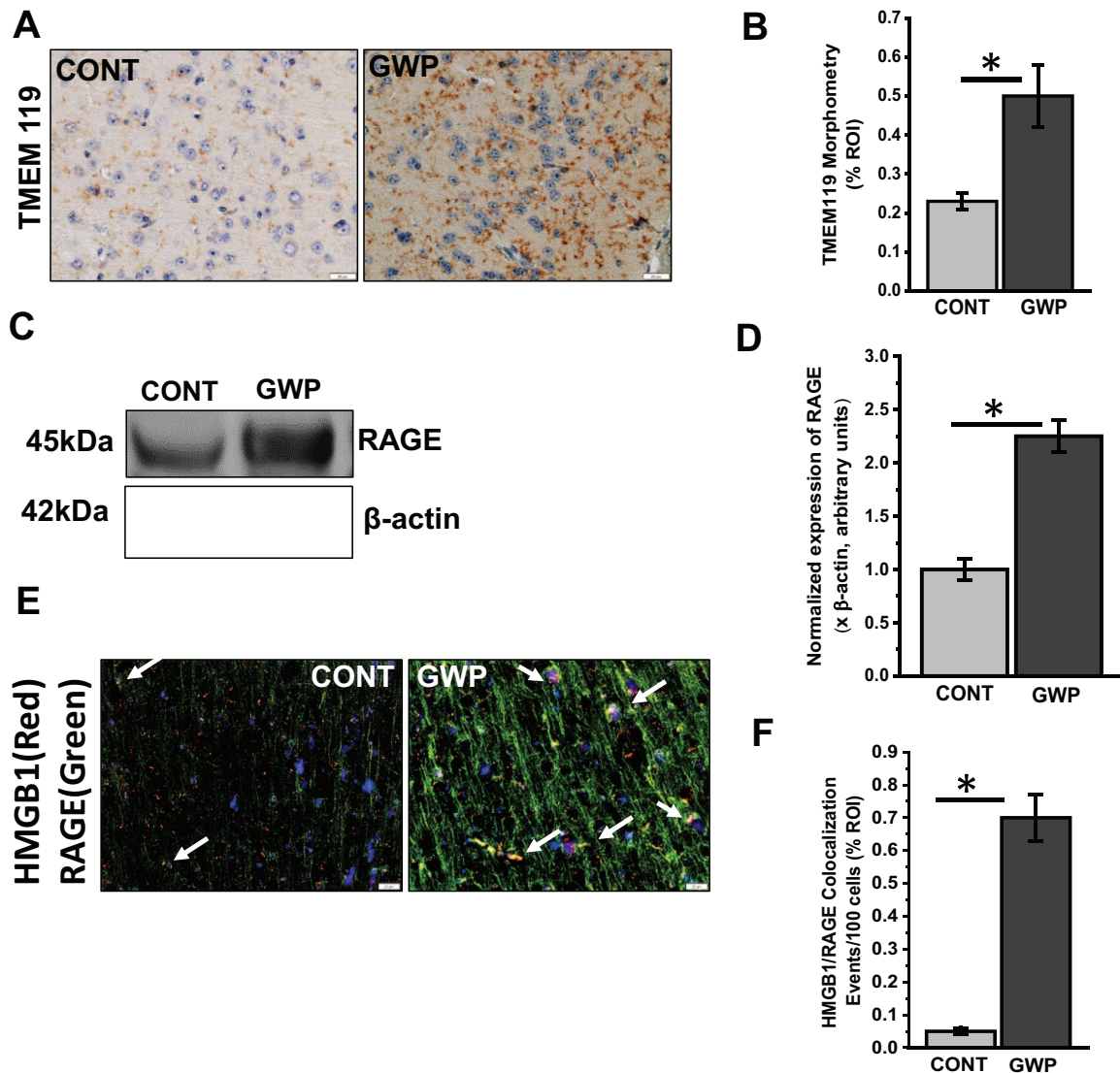


Figure 3. Activation of macrophages and associated HMGB1/RAGE complex formation. (A) TMEM119 immunoreactivity in frontal cortex. Representative immunohistochemistry micrographs of TMEM 119 reactivity in control (CONT) and GW chemical treated (GWP) mice (magnification 40× and scale bar 50 μm). (B) Morphometric analysis (represented as % ROI) obtained from 10 to 15 images from different microscopy fields from each mouse sample. Data are represented as mean ± SEM (* $P < .05$; $n = 6$). (C) Western blots of RAGE protein levels in the frontal cortex of GWP and CONT treated mice. (D) Morphometry analysis of all immunoblots normalized against β-actin ($n = 5$) (* $P < .05$; $n = 6$). Data are represented as mean ± SEM. (E) RAGE/HMGB1 complex formation. HMGB1 (labeled in red) and RAGE (labeled in green) and DAPI stained nucleus (labeled in blue) in GWP and CONT mice. Colocalizations are shown as yellow dots and marked with arrows in the micrographs (magnification 40× and scale bar 20 μm). See Supplemental Figure S3 for images of separate channels. (F) Morphometric analysis (represented as % ROI) obtained from 6 to 8 images from different microscopy fields from each mouse sample. Data are represented as mean ± SEM. (* $P < .05$; $n = 6$). GW indicates Gulf War; SEM, standard error of the mean; ROI, region of interest.

generation, eg, peroxynitrite, which reacts with tyrosine in proteins to form the stable adduct 3-nitrotyrosine. In Figure 4A and B, we detected significantly higher levels 3-nitrotyrosine (3NT) in GW chemical treated mice (GWP) compared with vehicle control treated mice (CONT); (* $P = .01$; $n = 6$). We also found that mice exposed to GW chemicals had significantly higher inflammasome activation compared with vehicle control treated mice (CONT) Figure 4C and D (* $P < .001$; $n = 6$). This activation was detected as yellow dots indicating a colocalization between the NLRP3 protein complex (labeled with red antibody) and the adapter protein ASC2 (marked with green), which facilitate the processing of pro-inflammatory

cytokines from their basal inactive to more active form via protein cleavage.

*Exposure to GW chemicals, decreased abundance of *A. muciniphila* is associated with a persistently increased neuroinflammation and low levels of BDNF*

Inflammasomes are large immune complexes found in several cell types and are responsible for processing the inflammatory cytokines IL-1β and IL-18 by cleaving them from their precursors.⁴⁰ Uncontrolled activation of these complexes can lead to chronic inflammation, as has been found in cancer, diabetes,

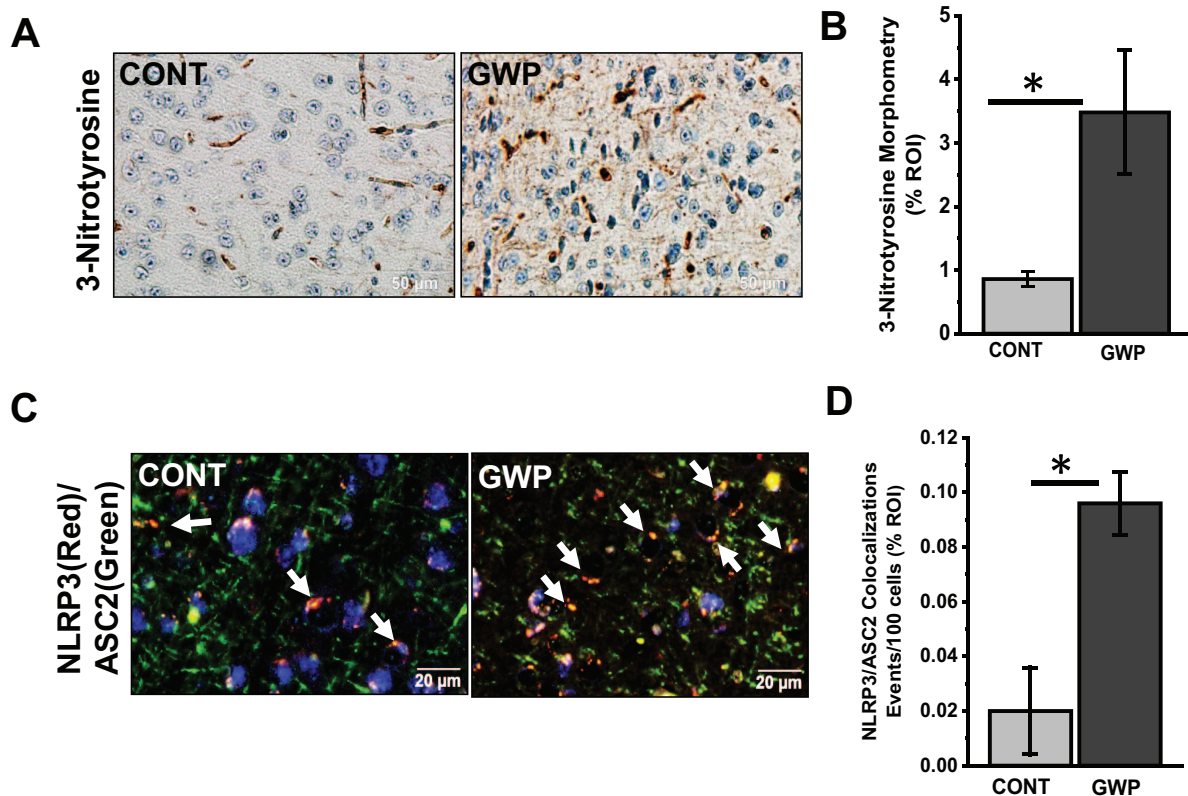


Figure 4. Increased ROS is associated with NLRP3 inflammasome activation. (A) 3-nitrotyrosine immunoreactivity in frontal cortex. Representative immunohistochemistry micrographs of 3-nitrotyrosine reactivity in control (CONT) and GW chemical treated (GWP) mice (magnification 40 \times and scale bar 50 μ m). (B) Morphometric analysis (represented as % ROI) obtained from 10 to 15 images from different microscopy fields from each mouse sample. Data are represented as Mean \pm SEM ($*P < .05$; $n = 6$). (C) Immunofluorescence micrographs showing activation of NLRP3 inflammasome protein. NLRP3 (labeled red) ASC2 (labeled in green) and DAPI stained nucleus (labeled in blue) in GWP and CONT mice. Colocalizations are shown as yellow dots and marked with arrows in the micrographs. See Supplemental Figure S4 for images of separate channels. Magnification 60 \times and scale bar 20 μ m. (D) Morphometric analysis (represented as % ROI) obtained from 6 to 8 images from different microscopy fields from each mouse sample. Data are represented as mean \pm SEM ($*P < .05$; $n = 6$). GW indicates Gulf War; ROS, reactive oxygen species; SEM, standard error of the mean; ROI, region of interest.

and neurodegenerative disease.^{41–44} In our study, we found that NLRP3 inflammasome activation was also significantly associated with increased IL-1 β (Figure 5A and B; $P = .001$, $n = 6$), IL-18 (Figure 5C and D; $P = .021$, $n = 6$), and IL-6 (Figure 5E and F; $P = .01$, $n = 6$) protein levels in GWP mouse frontal cortex when compared with mice treated with only vehicle control (CONT) (Figure 5A and F). Neurodegenerative diseases are often characterized by neuroinflammation, accompanied by decreased levels of neurotrophins.^{18,45} Similarly, in this study, we observed that mice which were treated with GW chemicals had significantly lower levels of the neurotrophin BDNF when compared with mice treated with only vehicle control (CONT) (Figure 5G and H, $P = .018$ and Figure 5I and J, $P = .001$, $n = 6$).

A muciniphila relative abundance correlates with BDNF levels and persistent neuroinflammation

A high abundance of *A muciniphila* has been linked to decreased inflammation in chronic diseases.^{38,46,47} To study whether the host bacteria's abundance played a role in affecting chronic inflammation and sustained BDNF levels in our model of GWI, we carried out correlative analyses to determine whether

there were statistically significant relationships between the bacterial abundance, inflammation, and BDNF levels. The results showed that there was a significant positive correlation between BDNF levels and abundance of *A muciniphila* (Pearson's $r = 0.83$, R^2 COD = 0.73; $P = .0024$), and a significant negative correlation with IL-1 β protein levels (Pearson's $r = -0.684$; R^2 COD = 0.46; $P = .02$) (Figure 6A and B). Shaded area represents 95% confidence bands.

Deletion of NLRP3 is protective against persistent systemic and neuroinflammation and is associated with an increase in BDNF levels

To study the role of NLRP3 in driving inflammation and lowering BDNF levels, we treated mice lacking NLRP3 with GW chemicals and then subjected them to our experimental conditions for 20 weeks or 5 months. We then studied the protein levels of IL-1 β , IL-18, IL-6, and BDNF by western blot analysis and immunohistochemistry. Our results show that there were significantly lower levels of IL-1 β (Figure 7A and E; $P = .006$, $n = 6$), IL-18 (Figure 7B and F; $P = .01$, $n = 6$), IL-6 (Figure 7C and G; $P = .015$, $n = 6$), and increased BDNF

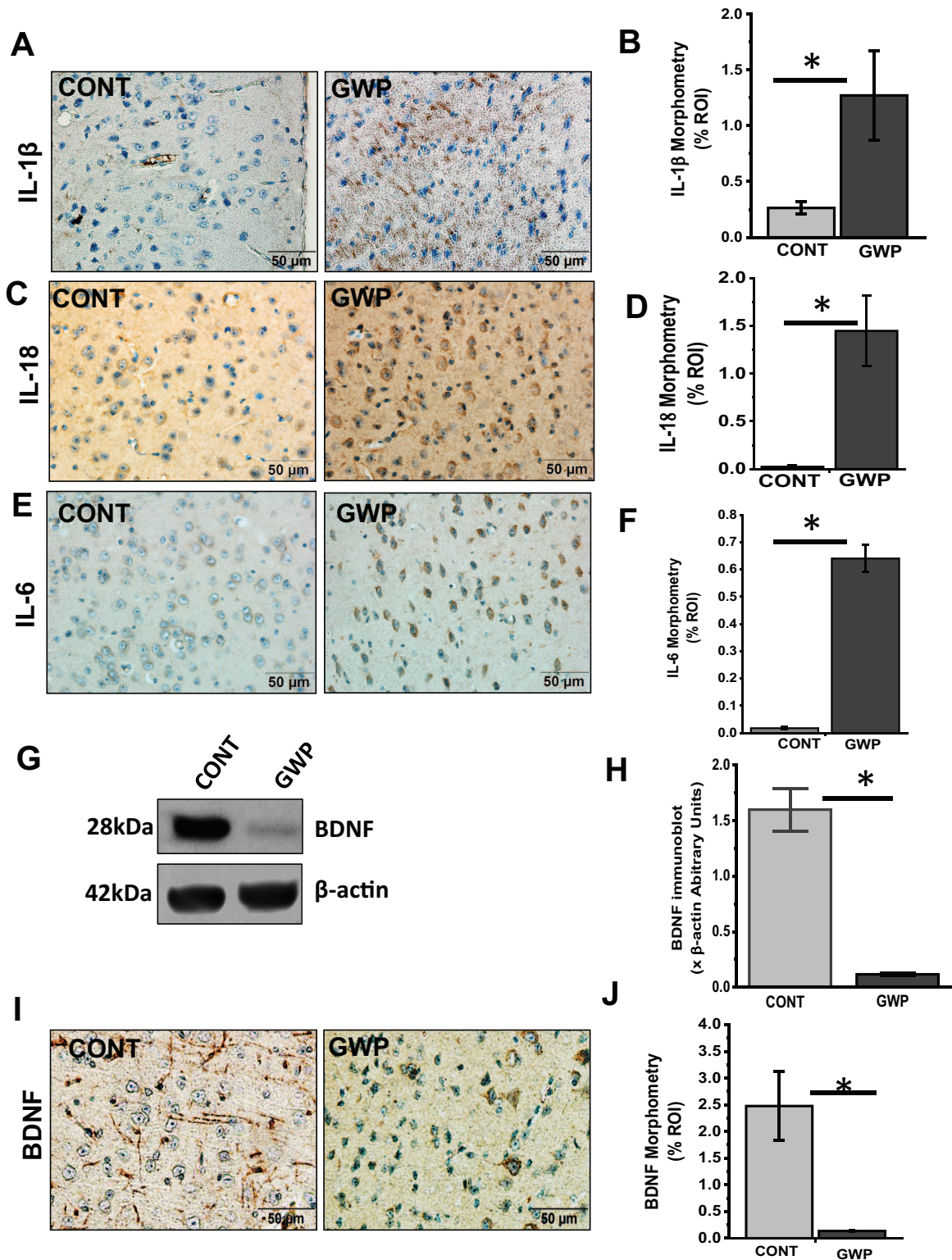


Figure 5. GW chemical exposure is associated with chronic neuroinflammation and decreased brain-derived neurotrophic factor (BDNF) levels in frontal cortex. (A, C, E) Immunohistochemistry micrographs of frontal cortex tissues of GWP and CONT treated mice showing immunoreactivity of IL-1 β , IL-18, and IL-6 (magnification 20 \times and scale bar 50 μ m). (B, D, F) Morphometric analysis (as % ROI) obtained from 10 to 15 images from different microscopic fields from each mouse sample. ($*P < .05$; $n=6$). Data are represented as mean \pm SEM. (G) Western blots of BDNF protein levels in the frontal cortex of GWP and CONT treated mice. (H) Morphometry analysis of immunoblots normalized against β -actin ($n=5$) ($*P < .05$; $n=5$). Data are represented as mean \pm SEM. (I) BDNF immunoreactivity. Representative immunohistochemistry micrographs showing BDNF in frontal cortex tissues of GWP and CONT treated mice (magnification 40 \times and scale bar 50 μ m). (J) Morphometric analysis (represented as % ROI) obtained from 10 to 15 images from different microscopy fields from each mouse sample ($*P < .05$; $n=6$). Data are represented as mean \pm SEM. BDNF indicates brain-derived neurotrophic factor; GW, Gulf War; SEM, standard error of the mean; ROI, region of interest.

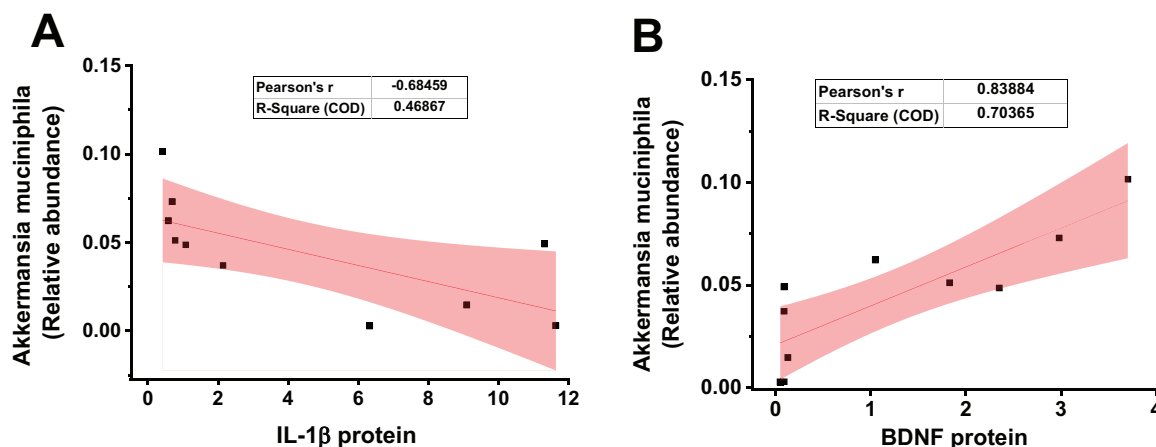


Figure 6. The decreased relative abundance of *Akkermansia muciniphila* correlates with IL-1 β and BDNF levels in the frontal cortex. (A) Correlation between *Akkermansia muciniphila* and IL-1 β levels in GW chemical (GWP) and vehicle control (CONT) treated mice. We carried out a linear regression analysis to determine the relationship between IL-1 β and *Akkermansia muciniphila* in GWP and CONT mice. There was a negative correlation between *Akkermansia muciniphila* and IL-1 β in the FC (Pearson's $r = -0.68$; R^2 COD = 0.46 and $P = .02$). (B) Correlation between *Akkermansia muciniphila* and BDNF levels in GW chemical (GWP) and vehicle control (CONT) treated mice. We carried out a linear regression analysis to determine the relationship between BDNF and *Akkermansia muciniphila* in GWP and CONT mice. There was a positive correlation between *Akkermansia muciniphila* relative abundance and BDNF levels (Pearson's $r = 0.83$, R^2 COD = 0.7 and $P = .0024$). BDNF indicates brain-derived neurotrophic factor; GW, Gulf War; COD, coefficient of dispersion.

(Figure 7D and H; $P = .007$, and Figure 7I and J; $P = .017$, $n = 6$) levels in the frontal cortex of NLRP3 KO mice treated with GW chemicals (GWP-NLRP3KO), when compared with wild type mice treated with GW chemicals (GWP). Furthermore, we studied systemic inflammation levels in the three groups of mice by analyzing serum IL-1 β (Figure 8A; $P = .046$, $n = 6$), TNF- α (Figure 8B; $P = .032$, $n = 6$) and IL-6 (Figure 8C; $P = .042$, $n = 6$) levels using an ELISA. Our results show that there is significantly lower inflammation in NLRP3KO mice treated with GW chemicals (GWP-NLRP3KO) compared with mice treated with GW chemicals (GWP).

Discussion

In our previous studies, we reported that there was a general alteration in microbiome accompanied by endotoxemia, a leaky gut, and inflammation in different organs such as the small intestine, brain, and liver.³⁰⁻³² We found significant increases in phyla Firmicutes and Tenericutes over Bacteroidetes in GW chemical exposed mice when compared with controls.³¹ However, it was not clear whether these alterations persisted long after GW chemical exposure or would eventually resolve over time through the repopulation and reconstitution of the host microbiome. We also were eager to study the mechanisms that would connect the altered microbiome and the persistent inflammatory changes in the intestine and the neural-immune network. In this study, mice were exposed to the GW chemicals and allowed to ad libitum diet and water for 20 weeks. This was to simulate the period of exposure (during the GW) and the subsequent period following their return from the war. We found that exposure to GW chemicals (the pesticide permethrin and prophylactic drug PB) in mice resulted in persistent pathology characterized by the low abundance of *Akkermansia muciniphila*, high circulatory HMGB1 levels, BBB dysfunction,

neuroinflammation, and lowered neurotrophin BDNF levels. Our findings and the proposed mechanism are summarized as a schematic illustration in Figure 9.

We report that exposure to GW chemicals caused a decrease in *Akkermansia muciniphila* or resulted in conditions that favor other bacteria populations repopulate over *Akkermansia muciniphila* (Figure 1A). *Akkermansia muciniphila* is a mucin degrading bacterium which exists as part of the normal human gut flora and is abundant in healthy individuals.⁴⁷⁻⁵⁰ In recent years, the herein reported bacterium is emerging as an important probiotic which can be consumed to improve health.⁵¹ This bacterium was found to improve ulcerative colitis in mice⁵² and restored colonic mucus layer thickness with decreased inflammation in aging mice.⁵³ In another study, the abundance of this bacterium inversely correlated with inflammation and altered lipid metabolism in obese mice.⁵¹ Although the mechanism by which *Akkermansia muciniphila* promotes these health benefits is not fully understood, studies report that the bacterium strengthens gut barrier integrity through its association with enterocytes and also produces high amounts of anti-inflammatory cytokine IL-8.^{48,54} It is possible that the low levels of this bacterium in the gut compromised gut barrier integrity, a condition that we have observed in our previous acute models of GWI.^{29,31} This condition of compromised gut barrier integrity has also been reported among veterans who suffer from gastrointestinal problems in GWI.⁵⁵ Moreover, a recent study by Janulewicz et al⁵⁶ showed that GWI afflicted veterans with gastrointestinal disturbances present gut dysbiosis among bacteria of the phylum Verrucomicrobia. Interestingly, *Akkermansia muciniphila* belongs to the same phylum. Another study found that *Akkermansia muciniphila* treatment normalized diet-induced metabolic endotoxemia, adiposity, and the adipose tissue marker CD11c in obese mice, which otherwise had increased inflammatory indicators in the intestine and aided in

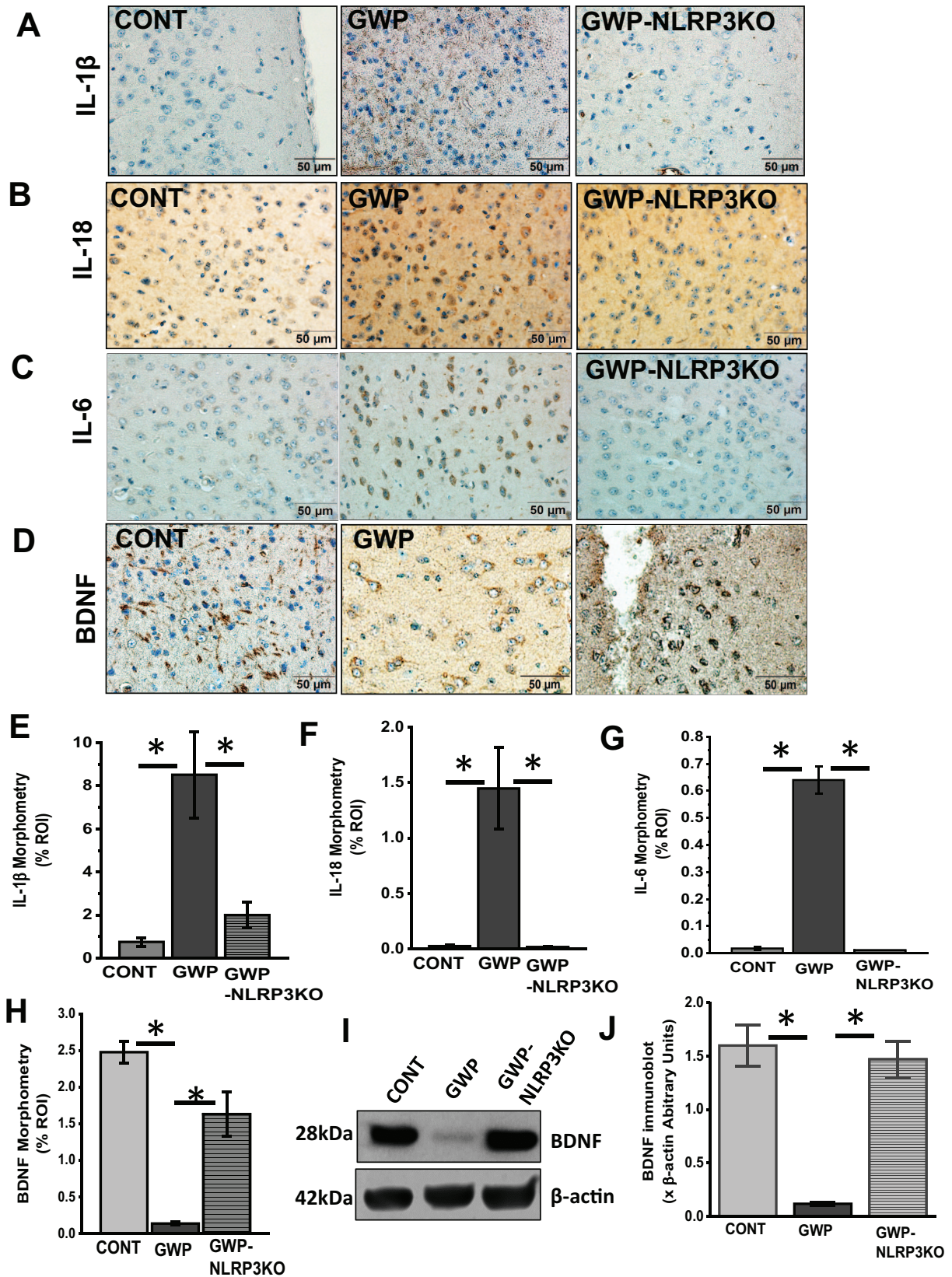


Figure 7. Deletion of NLRP3 is associated with decreased neuroinflammation and lower BDNF levels. (A to D) IL-1 β , IL-18, IL-6, and BDNF immunoreactivity in the frontal cortex. Representative immunohistochemistry micrographs showing IL-1 β , IL-18, IL-6, and BDNF, respectively, in frontal cortex tissues of GW chemical treated (GWP), GW chemical treated NLRP3KO (GWP-NLR3KO), and vehicle control (CONT) treated mice (magnification 40 \times and scale bar 50 μ m). (E to H) Morphometric analysis (represented as % ROI) obtained from 10 to 15 images from different microscopy fields from each mouse sample. Data are represented as mean \pm SEM. (* P < .05, n=6). (I) Western blots of BDNF protein levels in the frontal cortex of GWP and CONT treated mice. (J) Morphometry analysis of all immunoblots normalized against β -actin. Data are represented as mean \pm SEM (* P = .05, n=5). BDNF indicates brain-derived neurotrophic factor; GW, Gulf War; SEM, standard error of the mean.

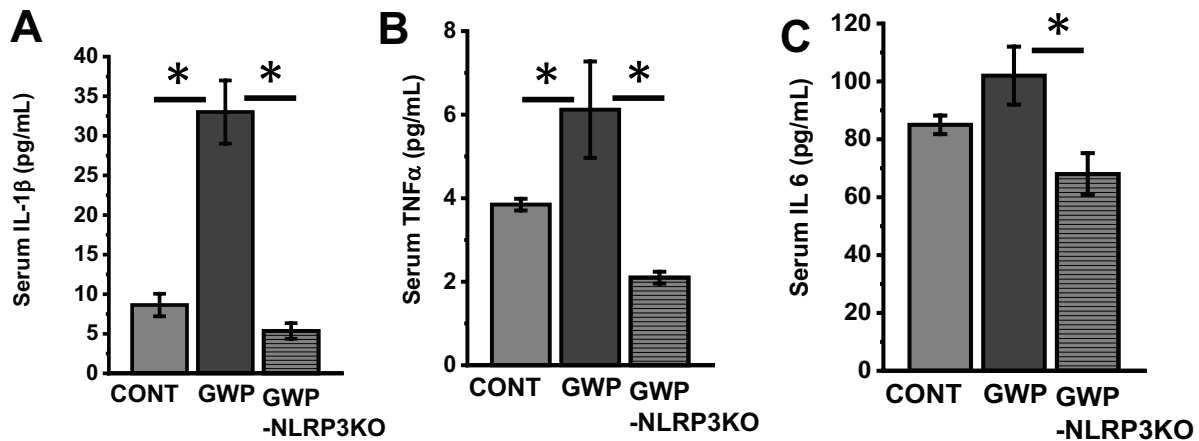


Figure 8. Deletion of NLRP3 is associated with decreased serum cytokine levels. (A to C) Serum cytokine levels. IL-1 β , TNF- α , and IL-6 levels, respectively, determined by ELISA in the serum of vehicle control (CONT), GW chemical treated (GWP) and GW chemical treated NLRP3KO mice (GWP-NLRP3KO). Data are represented as mean \pm SEM (* P < .05, n = 6). GW indicates Gulf War; SEM, standard error of the mean.

the metabolic disease development.⁴⁶ Similarly, our studies of GWI mouse models have consistently found that altered levels of tight junction proteins in the gut was associated with increase in endotoxins and DAMPs such as HMGB1 and inflammation that was related to an alteration of gut microbiome abundance.^{29,32} Notably, mice in the present study (using a persistence model of GWI) that were exposed to similar chemicals showed a slight increase in serum endotoxin levels (low-level endotoxemia consistent with an obesity phenotype) in GW chemical treated mice when compared with vehicle control treated mice (Supplemental Figure S1). In addition, a significant increase in circulatory HMGB1 levels was observed in GW chemical exposed mice which negatively correlated with *A muciniphila* relative abundance (Figure 1C to E) suggesting that a sustained and consistent low inflammatory trigger was closely associated with a persistent change in the microbiome and decreased *A Muciniphila* abundance in these mice. Furthermore, the persistence of systemic inflammatory indicators such as pro-inflammatory cytokines, eg, IL-1 β , IL-6, and TNF- α (Figure 8A to C), endotoxin levels and serum HMGB1 for such a long period that failed to ease even 20 weeks after exposure (equivalent to > 20 human years) and its connection with an altered microbiome triggered our interest to study their effects on neuronal structures and their networks.

Before we could study the neuroinflammatory indicators for persistence, we needed to assess the integrity of the BBB, a vital interface of neuronal physiology and pathology. Interestingly, our results showed that the expression of Claudin 5, a critical tight junction protein of the BBB in the brain, was decreased in the frontal cortex of mice treated with GW chemicals compared with controls (Figure 2A to E). This protein, together with others such as Claudin 1, zona occludens, and occludins make up tight junctions in the BBB. The BBB is a selective barrier found at the interface of blood vessels in the brain and brain tissue. It is made of a single cell layer of endothelial cells, astrocyte, and pericytes. Its unique properties allow it to tightly

regulate the movement of particles between the circulation and brain tissue.^{57,58} Claudin 5 and other tight junction proteins are found between adjacent endothelial cells of blood vessels and help to anchor these cells to create a tightly regulated selective barrier that allows the passage of particles between the blood and the brain.⁵⁹ Low levels of this protein have been found in neurodegenerative and neuroinflammatory diseases such as AD, PD, and schizophrenia.^{60,61} We found decreased mRNA and protein levels of this protein in GWP mice compared with controls (Figure 2A to E). This provides strong evidence that at least one key component of the BBB is dysregulated and this possibly compromised the barrier's integrity, likely caused by the serum mediators endotoxins, HMGB1, and pro-inflammatory cytokines causing it to become leaky. However, we have no direct evidence of such an event in an in vitro experimental setup using BBB endothelial cells. We hypothesized that this leaky BBB allowed the passage of unwanted particles such as DAMPs and PAMPS, HMGB1, as one such example, which we found to be greatly increased in the serum. It is also worth noting that even though serum endotoxin levels are not significantly higher in GWP mice compared with controls, even low levels of endotoxins over a long time can be a toxic stimulus to the body and may contribute to observed pathology.^{62,63}

HMGB1 is a DAMP known to trigger proinflammatory pathways through toll-like receptors (TLRs), eg, TLR4, and through the receptor for advanced glycation end products (RAGE).^{64,65} We found that there was increased activation of microglia in GWP mice compared with controls (Figure 3A and B) with an increased expression of RAGE receptors in the frontal cortex (Figure 3C and D). We also detected HMGB1/RAGE complex formation using immunofluorescence microscopy, which may indicate activation of RAGE signaling (Figure 3E and F). The activation of this pathway is known to result in the transcription of pro-inflammatory cytokines and the generation of ROS⁶⁶ such as nitric oxide. High levels of nitric oxide in the presence of superoxide could result in the formation of

peroxynitrite, a potent ROS which attacks tyrosine to form 3 nitrotyrosine denaturing them and rendering them dysfunctional. We found significantly higher levels of ROS in our GWP mice compared with controls (Figure 4A and B). High amounts of ROS are a known trigger of the NLRP3 inflammasome.⁶⁷ Inflammasomes are large protein complexes that are assembled in response to infections, etc, and are involved in the processing of pro-inflammatory cytokines such as IL-1 β and IL-18. We found that mice treated with GW chemicals had higher expression of NLRP3/ASC2 complex formation compared with controls (Figure 4C and D). Although inflammasomes are triggered as a defense mechanism, chronic activation of these complexes has been implicated in conditions characterized by chronic low-grade inflammation such as diabetes, PD, and ALS.^{68,69} This activation of the NLRP3 inflammasomes was followed by increased IL-1 β and IL-18 levels in the brain (Figure 5A to D), which might contribute to the persistent neuroinflammation in GWI.

In neurological diseases, inflammation has been associated with poor neuronal health, with fewer neurons, decreased neuronal plasticity, and growth.⁷⁰ This in part is due to low levels of neurotrophins such as BDNF. BDNF is a neurotrophin produced by neurons and is involved in neuronal growth, survival, and plasticity.²³ Studies by Guan and Fang, and another by Lapchak, suggest that increased IL-1 β levels interfered with BDNF synthesis,^{71,72} while Tong et al showed that increased IL-1 β interfered with BDNF signaling through the PI3K/AKT pathway by preventing its activation of AKT. The above mechanisms resulted in decreased growth and survival of neurons.⁷³ In this study, we report low levels of BDNF in the frontal cortex of mice, which were treated with GW chemicals compared with controls even 5 months post-exposure (Figure 5F and G). We also studied any correlations that BDNF, IL-1 β with *A muciniphila* relative abundance may have to connect the intestinal, microbiome changes, and neuronal levels of these mediators referenced above. In Figure 6A and B, we show that *A muciniphila* relative abundance correlated negatively with IL-1 β levels and positively with BDNF levels. The above result indicates that *A muciniphila* relative abundance might have played a role in modulating neuroinflammation and neurotrophin levels in GWI as has been the case in obesity and other diseases described previously.⁴⁶ This could be through the bacterium's production of anti-inflammatory compounds that counter inflammation or modulation of the intestinal barrier integrity. However, more studies need to be done to determine the exact mechanism. Finally, to study the role of NLRP3 inflammasome in contributing to neuroinflammation that persists for a prolonged period and its association with increased abundance of Akkermansia, we used a mouse model with the systemic knockout of NLRP3 gene (KO mouse). The results found that the deletion of this gene was associated with increased BDNF levels and protected the mice from neuroinflammation (Figure 7A to J). Deleting NLRP3 is protective

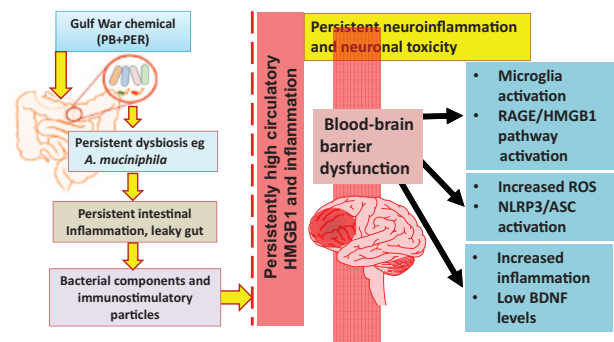


Figure 9. Schematic illustration of the proposed mechanism for persistent neuroinflammatory pathology in current study.

through preventing inflammasome activation and subsequent processing of pro-inflammatory cytokines and distinctly proves that the persistent inflammation in GWI chemical exposed mice that had altered *A muciniphila* abundance is due to NLRP3-mediated inflammasome activation though there may be multiple molecular mediators for triggering such an activation. Our current study identifies some of these mediators such as gut-derived endotoxins, HMGB1, or peroxynitrite, to name a few. Still, the molecular mechanism of such a trigger remains speculative currently.

In conclusion, we report that persistence of GWI inflammatory symptoms is characterized by low relative abundance of *A muciniphila* and chronic high circulatory HMGB1 levels which trigger NLRP3 mediated neuroinflammation and decreased levels of neurotrophins through RAGE signaling as shown in Figure 9. These findings not only provide insight into the mechanism of persistent neurological disturbances in GWI but also provide possible therapeutic targets. First, the microbiome can be targeted through replacement or enhancing of *A muciniphila* gut bacterial populations and other significantly lowered probiotic bacteria, and second, through therapies that target RAGE signaling or NLRP3 inflammasomes to relieve persistent inflammation and improve quality of life of veterans who suffer from GWI veterans.

Acknowledgements


We are grateful to the Instrument Resource Facility (University of South Carolina School of Medicine) and AML Labs (Baltimore MD) for providing excellent technical services. We are also thankful to Cosmos ID (Microbial Genomic Platform, Rockville, MD, USA) for their analysis of the bacteriome.

Author Contributions

SC conceived research, SC, DK and DB designed research. DK, DB, RS, AM, PS performed research. KS, PJ, SL, RH, NK and SC analyzed and interpreted data. DK, DB and SC drafted

manuscript, SC wrote, edited and approved final version of the manuscript.

ORCID iD

Saurabh Chatterjee  <https://orcid.org/0000-0003-1649-7149>

Supplemental Material

Supplemental material for this article is available online.

REFERENCES

- White RF, Steele L, O'Callaghan JP, et al. Recent research on Gulf War illness and other health problems in veterans of the 1991 Gulf war: effects of toxicant exposures during deployment. *Cortex*. 2016;74:449-475.
- Rose MR, Brix KA. Neurological disorders in Gulf War veterans. *Philos Trans R Soc Lond B Biol Sci*. 2006;361:605-618.
- Fukuda K, Nisenbaum R, Stewart G, et al. Chronic multisymptom illness affecting Air Force veterans of the Gulf War. *JAMA*. 1998;280:981-988.
- Engdahl BE, James LM, Miller RD, et al. Brain function in Gulf War illness (GWI) and Associated Mental Health comorbidities. *J Neurol Neuromedicine*. 2018;3:24-34.
- Jeffrey MG, Kregel M, Kibler JL, et al. Neuropsychological findings in Gulf War illness: a review. *Front Psychol*. 2019;10:2088.
- Doebbeling BN, Clarke WR, Watson D, et al. Is there a Persian Gulf War syndrome? Evidence from a large population-based survey of veterans and nondeployed controls. *Am J Med*. 2000;108:695-704.
- Gray GC, Kaiser KS, Hawksworth AW, Hall FW, Barrett-Connor E. Increased postwar symptoms and psychological morbidity among U.S. *Am J Trop Med Hyg*. 1999;60:758-766.
- The Persian Gulf experience and health. NIH Technology Assessment Workshop Panel. *JAMA*. 1994;272:391-396.
- Golomb BA. Acetylcholinesterase inhibitors and Gulf War illnesses. *Proc Natl Acad Sci USA*. 2008;105:4295-4300.
- Joshi U, Pearson A, Evans JE, et al. A permethrin metabolite is associated with adaptive immune responses in Gulf War illness. *Brain Behav Immun*. 2019;81:545-559.
- Brimfield AA. Chemicals of military deployments: revisiting Gulf War syndrome in light of new information. *Prog Mol Biol Transl Sci*. 2012;112:209-230.
- Mawson AR, Croft AM. Gulf War illness: unifying hypothesis for a continuing health problem. *Int J Environ Res Public Health*. 2019;16:1111.
- Van Riper SM, Alexander AL, Koltyn KF, et al. Cerebral white matter structure is disrupted in Gulf War veterans with chronic musculoskeletal pain. *Pain*. 2017;158:2364-2375.
- Abou-Donia MB, Conboy LA, Kokkotou E, et al. Screening for novel central nervous system biomarkers in veterans with Gulf War illness. *Neurotoxicol Teratol*. 2017;61:36-46.
- Zakirova Z, Tweed M, Crynen G, et al. Gulf War agent exposure causes impairment of long-term memory formation and neuropathological changes in a mouse model of Gulf War illness. *PLoS ONE*. 2015;10:e0119579.
- Madhu LN, Attaluri S, Kodali M, et al. Neuroinflammation in Gulf War illness is linked with HMGB1 and complement activation, which can be discerned from brain-derived extracellular vesicles in the blood. *Brain Behav Immun*. 2019;81:430-443.
- Khan N, Smith MT. Neurotrophins and neuropathic pain: role in pathobiology. *Molecules*. 2015;20:10657-10688.
- Jiao SS, Shen LL, Zhu C, et al. Brain-derived neurotrophic factor protects against tau-related neurodegeneration of Alzheimer's disease. *Transl Psychiatry*. 2016;6:e907.
- Sampaio TB, Savall AS, Gutierrez MEZ, Pinton S. Neurotrophic factors in Alzheimer's and Parkinson's diseases: implications for pathogenesis and therapy. *Neural Regen Res*. 2017;12:549-557.
- Allen SJ, Watson JJ, Dawbarn D. The neurotrophins and their role in Alzheimer's disease. *Curr Neuropharmacol*. 2011;9:559-573.
- Grande I, Fries GR, Kunz M, Kapczynski F. The role of BDNF as a mediator of neuroplasticity in bipolar disorder. *Psychiatry Investig*. 2010;7:243-250.
- Tome D, Fonseca CP, Campos FL, Baltazar G. Role of neurotrophic factors in Parkinson's disease. *Curr Pharm Des*. 2017;23:809-838.
- Lima Giacobbo B, Doorduyn J, Klein HC, Dierckx RAJO, Bromberg E, de Vries EFJ. Brain-derived neurotrophic factor in brain disorders: focus on neuroinflammation. *Mol Neurobiol*. 2019;56:3295-3312.
- Heneka MT, Carson MJ, El Khoury J, et al. Neuroinflammation in Alzheimer's disease. *Lancet Neurol*. 2015;14:388-405.
- Wang Q, Liu Y, Zhou J. Neuroinflammation in Parkinson's disease and its potential as therapeutic target. *Transl Neurodegener*. 2015;4:19.
- Lee Y, Lee S, Chang SC, Lee J. Significant roles of neuroinflammation in Parkinson's disease: therapeutic targets for PD prevention. *Arch Pharm Res*. 2019;42:416-425.
- Miranda M, Morici JF, Zanoni MB, Bekinschtein P. Brain-derived neurotrophic factor: a key molecule for memory in the healthy and the pathological brain. *Front Cell Neurosci*. 2019;13:363.
- Bathina S, Das UN. Brain-derived neurotrophic factor and its clinical implications. *Arch Med Sci*. 2015;11:1164-1178.
- Kimono D, Sarkar S, Albadrani M, et al. Dysbiosis-associated enteric glial cell immune-activation and redox imbalance modulate tight junction protein expression in Gulf War illness pathology. *Front Physiol*. 2019;10:1229.
- Seth RK, Maqsood R, Mondal A, et al. Gut DNA virome diversity and its association with host bacteria regulate inflammatory phenotype and neuronal immunotoxicity in experimental Gulf War illness. *Viruses*. 2019;11:968.
- Alhasson F, Das S, Seth R, et al. Altered gut microbiome in a mouse model of Gulf War illness causes neuroinflammation and intestinal injury via leaky gut and TLR4 activation. *PLoS ONE*. 2017;12:e0172914.
- Seth RK, Kimono D, Alhasson F, et al. Increased butyrate priming in the gut stalls microbiome associated-gastrointestinal inflammation and hepatic metabolic reprogramming in a mouse model of Gulf War illness. *Toxicol Appl Pharmacol*. 2018;350:64-77.
- Zakirova Z, Reed J, Crynen G, et al. Complementary proteomic approaches reveal mitochondrial dysfunction, immune and inflammatory dysregulation in a mouse model of Gulf War illness. *Proteomics Clin Appl*. 2017;11:1600190.
- Locker AR, Michalovic LT, Kelly KA, Miller JV, Miller DB, O'Callaghan JP. Corticosterone primes the neuroinflammatory response to Gulf War Illness-relevant organophosphates independently of acetylcholinesterase inhibition. *J Neurochem*. 2017;142:444-455.
- O'Callaghan JP, Kelly KA, Locker AR, Miller DB, Lasley SM. Corticosterone primes the neuroinflammatory response to DFP in mice: potential animal model of Gulf War illness. *J Neurochem*. 2015;133:708-721.
- Dao MC, Everard A, Aron-Wisniewsky J, et al. *Akkermansia muciniphila* and improved metabolic health during a dietary intervention in obesity: relationship with gut microbiome richness and ecology. *Gut*. 2016;65:426-436.
- Ottman N, Geerlings SY, Aalvink S, de Vos WM, Belzer C. Action and function of *Akkermansia muciniphila* in microbiome ecology, health and disease. *Best Pract Res Clin Gastroenterol*. 2017;31:637-642.
- Remely M, Hippe B, Zanner J, Aumueller E, Brath H, Haslberger AG. Gut microbiota of obese, type 2 diabetic individuals is enriched in *Faecalibacterium prausnitzii*, *Akkermansia muciniphila* and *Peptostreptococcus anaerobius* after weight loss. *Endocr Metab Immune Disord Drug Targets*. 2016;16:99-106.
- Andreasson KI, Bachstetter AD, Colonna M, et al. Targeting innate immunity for neurodegenerative disorders of the central nervous system. *J Neurochem*. 2016;138:653-693.
- Latz E, Xiao TS, Stutz A. Activation and regulation of the inflammasomes. *Nat Rev Immunol*. 2013;13:397-411.
- Karan D. Inflammasomes: emerging central players in cancer immunology and immunotherapy. *Front Immunol*. 2018;9:3028.
- Lin C, Zhang J. Inflammasomes in inflammation-induced cancer. *Front Immunol*. 2017;8:271.
- Sepehri Z, Kiani Z, Afshari M, Kohan F, Dalvand A, Ghavami S. Inflammasomes and type 2 diabetes: an updated systematic review. *Immunol Lett*. 2017;192:97-103.
- Lang Y, Chu F, Shen D, et al. Role of inflammasomes in neuroimmune and neurodegenerative diseases: a systematic review. *Mediators Inflamm*. 2018;2018:1549549.
- Ng TKS, Ho CSH, Tam WWS, Kua EH, Ho RC. Decreased serum brain-derived neurotrophic factor (BDNF) levels in patients with Alzheimer's disease (AD): a systematic review and meta-analysis. *Int J Mol Sci*. 2019;20:257.
- Everard A, Belzer C, Geurts L, et al. Cross-talk between *Akkermansia muciniphila* and intestinal epithelium controls diet-induced obesity. *Proc Natl Acad Sci USA*. 2013;110:9066-9071.
- Cani PD, de Vos WM. Next-generation beneficial microbes: the case of *Akkermansia muciniphila*. *Front Microbiol*. 2017;8:1765.
- Geerlings SY, Kostopoulos I, de Vos WM, Belzer C. *Akkermansia muciniphila* in the human gastrointestinal tract: when, where, and how? *Microorganisms*. 2018;6:75.
- Zhang T, Li Q, Cheng L, Buch H, Zhang F. *Akkermansia muciniphila* is a promising probiotic. *Microb Biotechnol*. 2019;12:1109-1125.
- Lopez-Siles M, Enrich-Capo N, Aldeguer X, et al. Alterations in the abundance and co-occurrence of *Akkermansia muciniphila* and *Faecalibacterium prausnitzii* in the colonic mucosa of inflammatory bowel disease subjects. *Front Cell Infect Microbiol*. 2018;8:281.
- Schneeberger M, Everard A, Gomez-Valades AG, et al. *Akkermansia muciniphila* inversely correlates with the onset of inflammation, altered

- adipose tissue metabolism and metabolic disorders during obesity in mice. *Sci Rep.* 2015;5:16643.
52. Bian X, Wu W, Yang L, et al. Administration of *Akkermansia muciniphila* ameliorates dextran sulfate sodium-induced ulcerative colitis in mice. *Front Microbiol.* 2019;10:2259.
 53. van der Lugt B, van Beek AA, Aalvink S, et al. *Akkermansia muciniphila* ameliorates the age-related decline in colonic mucus thickness and attenuates immune activation in accelerated aging *Ercc1 (-/Delta7)* mice. *Immun Ageing.* 2019;16:6.
 54. Reunanen J, Kainulainen V, Huuskonen L, et al. *Akkermansia muciniphila* adheres to enterocytes and strengthens the integrity of the epithelial cell layer. *Appl Environ Microbiol.* 2015;81:3655-3662.
 55. Zhang B, Verne ML, Fields JZ, Verne GN, Zhou Q. Intestinal hyperpermeability in Gulf War veterans with chronic gastrointestinal symptoms. *J Clin Gastroenterol.* 2019;53:e298-e302.
 56. Janulewicz PA, Seth RK, Carlson JM, et al. The Gut-microbiome in Gulf War veterans: a preliminary report. *Int J Environ Res Public Health.* 2019;16:3751.
 57. Daneman R, Prat A. The blood-brain barrier. *Cold Spring Harb Perspect Biol.* 2015;7:a020412.
 58. Villabona-Rueda A, Erice C, Pardo CA, Stins MF. The evolving concept of the blood brain barrier (BBB): from a single static barrier to a heterogeneous and dynamic relay center. *Front Cell Neurosci.* 2019;13:405.
 59. Greene C, Hanley N, Campbell M. Claudin-5: gatekeeper of neurological function. *Fluids Barriers CNS.* 2019;16:3.
 60. Romanitan MO, Popescu BO, Spulber S, et al. Altered expression of claudin family proteins in Alzheimer's disease and vascular dementia brains. *J Cell Mol Med.* 2010;14:1088-1100.
 61. Nishiura K, Ichikawa-Tomikawa N, Sugimoto K, et al. PKA activation and endothelial claudin-5 breakdown in the schizophrenic prefrontal cortex. *Oncotarget.* 2017;8:93382-93391.
 62. Meessen ECE, Warmbrunn MV, Nieuwdorp M, Soeters MR. Human post-prandial nutrient metabolism and low-grade inflammation: a narrative review. *Nutrients.* 2019;11:3000.
 63. Netto Candido TL, Bressan J, Alfenas RCG. Dysbiosis and metabolic endotoxemia induced by high-fat diet. *Nutr Hosp.* 2018;35:1432-1440.
 64. Kokkola R, Andersson A, Mullins G, et al. RAGE is the major receptor for the proinflammatory activity of HMGB1 in rodent macrophages. *Scand J Immunol.* 2005;61:1-9.
 65. Chandrashekar V, Seth RK, Dattaroy D, et al. HMGB1-RAGE pathway drives peroxynitrite signaling-induced IBD-like inflammation in murine nonalcoholic fatty liver disease. *Redox Biol.* 2017;13:8-19.
 66. Weber DJ, Allette YM, Wilkes DS, White FA. The HMGB1-RAGE inflammatory pathway: implications for brain injury-induced pulmonary dysfunction. *Antioxid Redox Signal.* 2015;23:1316-1328.
 67. Abais JM, Xia M, Zhang Y, Boini KM, Li PL. Redox regulation of NLRP3 inflammasomes: ROS as trigger or effector? *Antioxid Redox Signal.* 2015;22:1111-1129.
 68. Ozaki E, Campbell M, Doyle SL. Targeting the NLRP3 inflammasome in chronic inflammatory diseases: current perspectives. *J Inflamm Res.* 2015;8:15-27.
 69. Davis BK, Wen H, Ting JP. The inflammasome NLRs in immunity, inflammation, and associated diseases. *Annu Rev Immunol.* 2011;29:707-735.
 70. Xie ZM, Wang XM, Xu N, et al. Alterations in the inflammatory cytokines and brain-derived neurotrophic factor contribute to depression-like phenotype after spared nerve injury: improvement by ketamine. *Sci Rep.* 2017;7:3124.
 71. Guan Z, Fang J. Peripheral immune activation by lipopolysaccharide decreases neurotrophins in the cortex and hippocampus in rats. *Brain Behav Immun.* 2006;20:64-71.
 72. Lapchak PA, Araujo DM, Hefti F. Systemic interleukin-1 beta decreases brain-derived neurotrophic factor messenger RNA expression in the rat hippocampal formation. *Neuroscience.* 1993;53:297-301.
 73. Tong L, Balazs R, Sojampornkul R, Thangnipon W, Cotman CW. Interleukin-1 beta impairs brain derived neurotrophic factor-induced signal transduction. *Neurobiol Aging.* 2008;29:1380-1393.